

GRANULITES OF NORTHERN KOREA

V.A. Glebovitsky, I.S. Sedova, S.A. Bushmin, Ye.A. Vapnik, A.K. Buiko

Institute of Precambrian Geology and Geochronology of Russia Academy of Science, emb. Makarova 2, St. Petersburg 199034, Russia

ABSTRACT : Granulite complexes in northern (the Nangnim block), eastern (the Kimchaek zone of the Macheonryong belt) and southern (separate windows among upper Proterozoic structures such as the Wonsan, Nampo and Haeju granulites) parts of the Northern Korea are studied. Multistage deformations, metamorphic and migmatitic events, and granite formations are recognized in these granulite complexes. Mineral thermobarometry and fluid inclusion investigations are used to establish the P-T evolutionary trends during prograde and retrograde metamorphic events. The peak metamorphism of granulites is characterized by temperature near 800°C and pressure near 5.5–6 kb. Retrograde evolution includes cooling at constant pressure or with variable pressure ranging up to 7–8 kb. This P-T change corresponds to the transition from high to moderate or low geothermal gradient. The subsequent cooling is accompanied by significant decompression to 3–4 kb.

Key words : Granulite, P-T-t path, fluid inclusion

INTRODUCTION

Granulites of North Korea are widespread in Archean and Proterozoic metamorphic complexes, systematic description of which was first published by A.A. Markakushev and his colleagues together with Korean geologists (1966). The granulites are preserved as tectonic blocks of variable sizes and as remnants with diffuse contacts within younger and lower grade units and granites. Together with the latter, they experienced different events, including ductile deformation and overprinting metamorphism, ultrametamorphism and granite formation. The aim of the present study is to establish P-T-time paths of granulites in order to understand the relationship and interactions of various geological processes responsible for the granulite formation.

GEOLOGICAL SETTING, METAMORPHISM, ULTRAMETAMORPHISM AND GRANITE FORMATION

In the northern part of North Korea, granulites are found within the Nangnim block and in the

eastern part of the Macheonryong block assigned as Kimchaek zone. In the southern part of North Korea, granulites form separate exposures, and are named according to neighbouring towns as the Wonsan, Nampo and Haeju granulites (Figs. 1 and 2).

Within the Nangnim block granulites occur as fragments either in granite-gneisses, tonalite-gneisses and nebulites, or in intrusive granitoids of the Rechvonsan and the Andor complexes, or migmatized gabbro-diorites. The Nangnim block is related to the North China granulite belt. Both are likely to form a chain of similar block aligned to the east-west direction, and divided by younger Proterozoic zones (Fig. 3) (Ren *et al.*, 1987; Field excursion, 1988). Two age groups of granulites are distinguished in the North China granulite belt: (1) 3430-3470 Ma (Qianxi group), and more commonly (2) 2650 Ma (Songwong group). Most probably, granulites of the Nangnim block are similar to the latter, because one of the early varieties of the Rechvonsan granitoid complex has a K-Ar age of 2039 Ma (Marakushev *et al.*, 1966). Recent data on Rb-Sr geochronology suggest that the la-

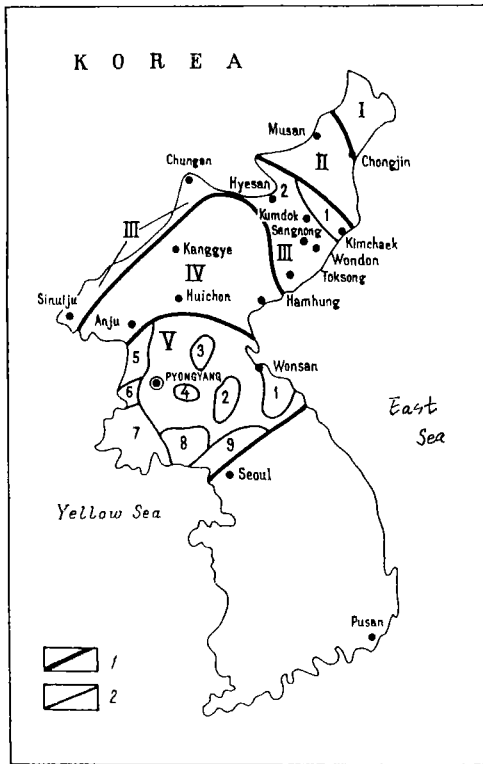


Fig. 1. Precambrian terranes of Northern Korea. 1, boundaries between main tectonic structures; 2, boundaries of the early Precambrian windows. On the map: I, Tumangang belt; II, Kwanmo depression; III, Macheonryong belt; IV, Nangnim block; V, Pyongyang depression; windows: 1, Wonsan; 2, Ichkhon; 3, Jandok; 4, Chamkol; 5, Chunsan; 6, Nampo; 7, Quail; 8, Haeju; 9, Kaeseong.

test high-grade metamorphic event occurred during the period from 1940 to 1820 Ma (Gorokhov *et al.*, 1993).

The Nangnim metamorphic complex consists of highly aluminous, biotite-garnet-cordierite gneiss (pelites) and moderately aluminous hypersthene-biotite-garnet gneiss (semi-pelites and greywackes) with layers of two pyroxene mafic schists, amphibolites, and dolomite marbles. In the Pusan region, Marakushev *et al.* (1966) observed gneisses containing the assemblage $\text{Gr} + \text{Opx} + \text{Cord} + \text{Kfsp} + \text{Pl} + \text{Qz}$, which characterizes the high-temperature subfacies of the granulite facies. Two assemblages: $\text{Gr} + \text{Opx} + \text{Bt} + \text{Kfsp} + \text{Pl} + \text{Qz}$

and $\text{Gr} + \text{Cord} + \text{Bt} + \text{Kfsp} + \text{Pl} + \text{Qz}$, corresponding to middle temperature $\text{Gr} + \text{Cord} + \text{Bt} + \text{Kfsp}$ subfacies of the granulite facies, are usually stable and widespread. The Mg mole fraction of garnet in cordierite-bearing gneisses seldom exceeds 0.3, and thus metamorphic conditions did not reach high-rank granulite facies in both temperature and pressure. This is the reason for the appearance of predominant assemblage in mafic rocks: $\text{Opx} + \text{Cpx} + \text{Pl}$ with high anorthite content (upto bytownite), established by Marakushev *et al.* (1966). Garnet is observed only in mafic rocks with high $\text{Fe}/\text{Fe} + \text{Mg}$ value, developed near the boundary between the Nangnim block and the Macheonryong belt. Diopside, forsterite and spinel together with quartz occur in dolomite marbles. Secondary assemblage of biotite and sillimanite occurs in garnet-cordierite gneisses, indicating either temperature drop or pressure increase.

Multistage prolonged evolution of the Nangnim complex can be traced by correlating deformation, migmatitization and granite formation. For example, in the Huichon region, the early, thin, stromatic migmatite leucosomes of inhomogeneous composition (enriched in either plagioclase or quartz or K-feldspar) are transected by the later and thicker (up to a centimeter wide) leucosomes of the garnet-bearing granites, and both leucosomes are deformed in isoclinal fold system (Fig. 4-1). Garnet infrequently forms prophyroblasts or clusters, which extend beyond leucosome veins (Fig. 4-2) and are surrounded by quartz. These clusters settle down obliquely to vein contacts. Cordierite-garnet-K-feldspar metasomatites cut these leucosomes. Charnokites and enderbite gneisses in the form of bands of patches are formed during this stage, replacing gneisses and mafic rocks, respectively (Fig. 4-3). They are often crosscut by garnet-bearing veins (Fig. 4-4). The earlier migmatites with thin leucosomes γ_1 and γ_2 (biotite- and garnet-bearing) are intersected by the veins of the hypersthene granites (γ_3) and biotite ones (γ_4). All these rocks undergo secon-

MAJOR TECTONIC STRUCTURES EAST CHINA AND KOREA

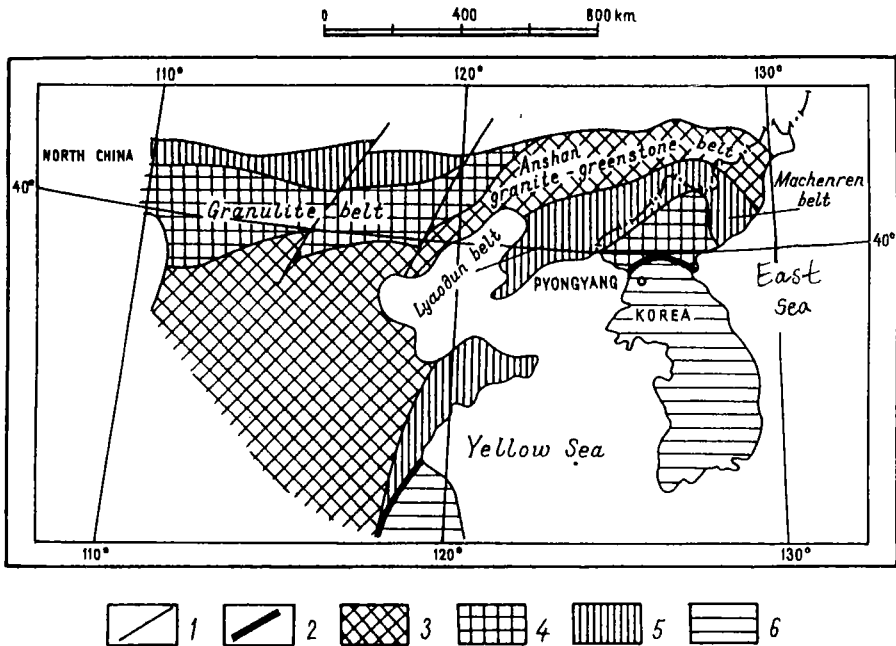


Fig. 2. The main tectonic structures of East China and Korea. 1, intracratonic boundaries of the main tectonic structures; 2, boundaries between Sino-Korean and South China cratons; 3-5, Sino-Korean craton: 3, Archaean granite-greenstone area; 4, Archaean granulite belt; 5, Early Proterozoic mobile belt; 6, South China craton.

dary shearing with granulite structure formation. Hypersthene, K-feldspar and other minerals are recrystallized. A little garnet-bearing homogeneous granite and enderbite bodies occur in polymigmatites. K-feldspar prophyroblasts replace hypersthene and plagioclase. Orthopyroxenes are rimmed by small garnet crystals formed during structural evolution. The marginal part of complex is subjected to strong shearing, accompanying the complete replacement of cordierite and plagioclase by mica aggregates, biotite porphyroblasts, quartz and plagioclase recrystallized. These facts testify that the granulite metamorphism, accompanied by folding, proceeded at least in two stages; the granulite facies conditions are preserved during all of the migmatitization and granite formation events. Amphibolite facies diaphoresis took place only after all these transformations.

Multistage migmatite formation is characteris-

tic for the Karlggye region, where earlier leucosomes of the stromatic migmatites in garnet-biotite and garnet-cordierite gneisses with quartzite gneiss layers are cut by thicker pygmatite veins of the garnet granite, containing pegmatoid and quartz zones and clusters, and by unfolded granite veins with garnet and cordierite (Fig. 4-5). The migmatites alternate with nebulites and granite-gneisses, including relics of the aluminous gneisses, biotite-plagioclase schists and quartzite-gneisses (Fig. 4-6). Recrystallized garnet grains develop as clusters and zones; garnet and cordierite aggregates are rimmed by quartz and plagioclase. There is a successive alternation of different compositional bands (enriched in cordierite, garnet, biotite, or tourmaline), either of gneissic or massive structure, and either of granoblastic or subhedral texture in granite gneisses. The latter also contains the patches of homog-

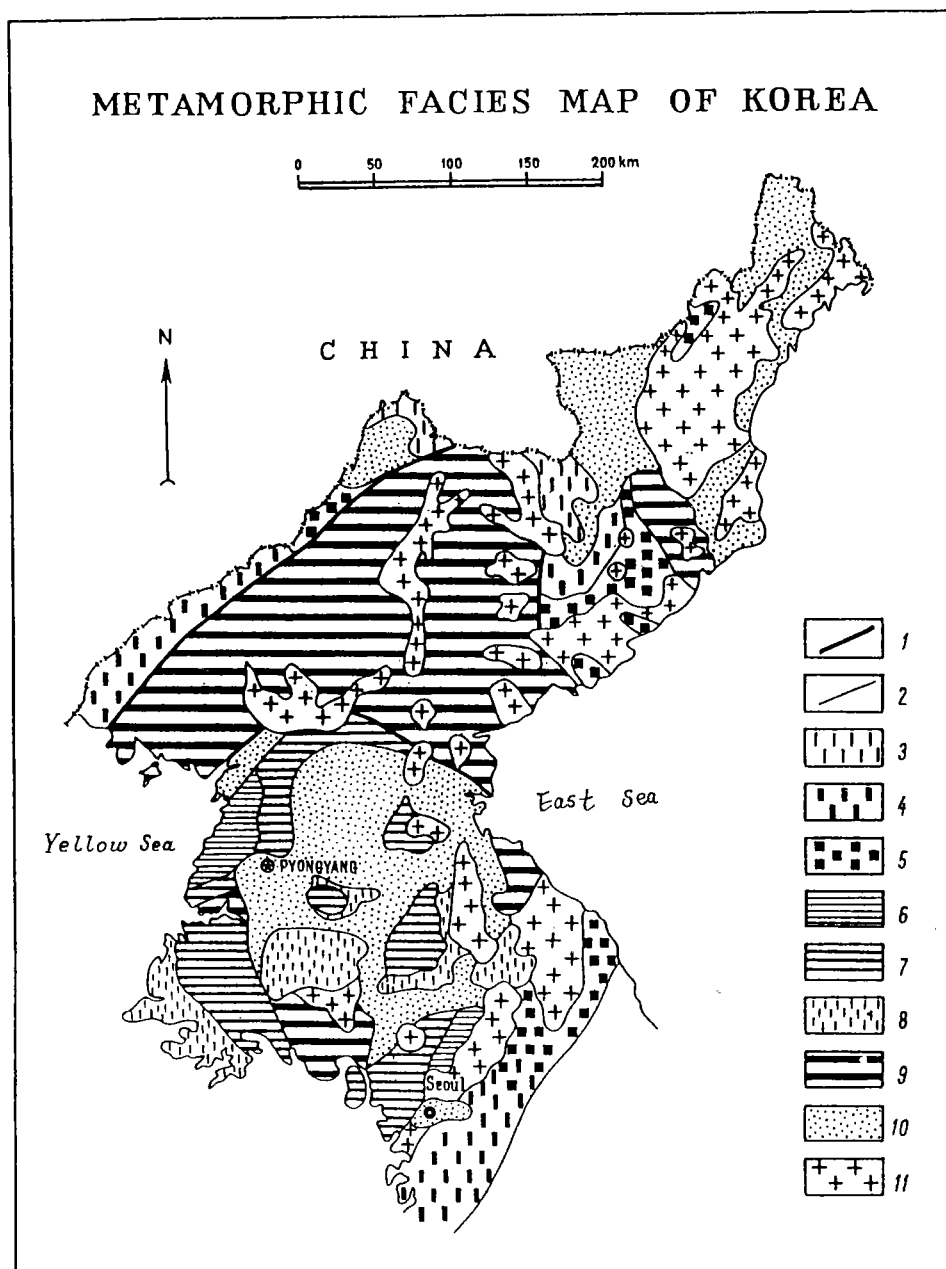


Fig. 3. The map of metamorphic facies of Northern Korea. 1, boundaries between main tectonic structures; 2, other geological and metamorphic boundaries; 3-5, andalusite-sillimanite facies series; 3, greenschist facies; 4, staurolite and andalusite-cordierite-biotite subfacies of epidote-amphibolite facies; 5, garnet-biotite-sillimanite subfacies of amphibolite facies; 6-7, kyanite-sillimanite facies series; 6, staurolite subfacies of epidote-amphibolite facies; 7, garnet-kyanite-biotite-muscovite subfacies of amphibolite facies; 8-9, facies of undefined pressure; 8, greenschist facies; 9, granulite facies; 10, Phanerozoic sediments; 11, intrusions.

neous and coarse-grained rocks of granitic composition with cross-cutting tongues. Similar rocks

form dikes with sharp contacts (Fig. 4-8). Such relationships can be considered as transition from

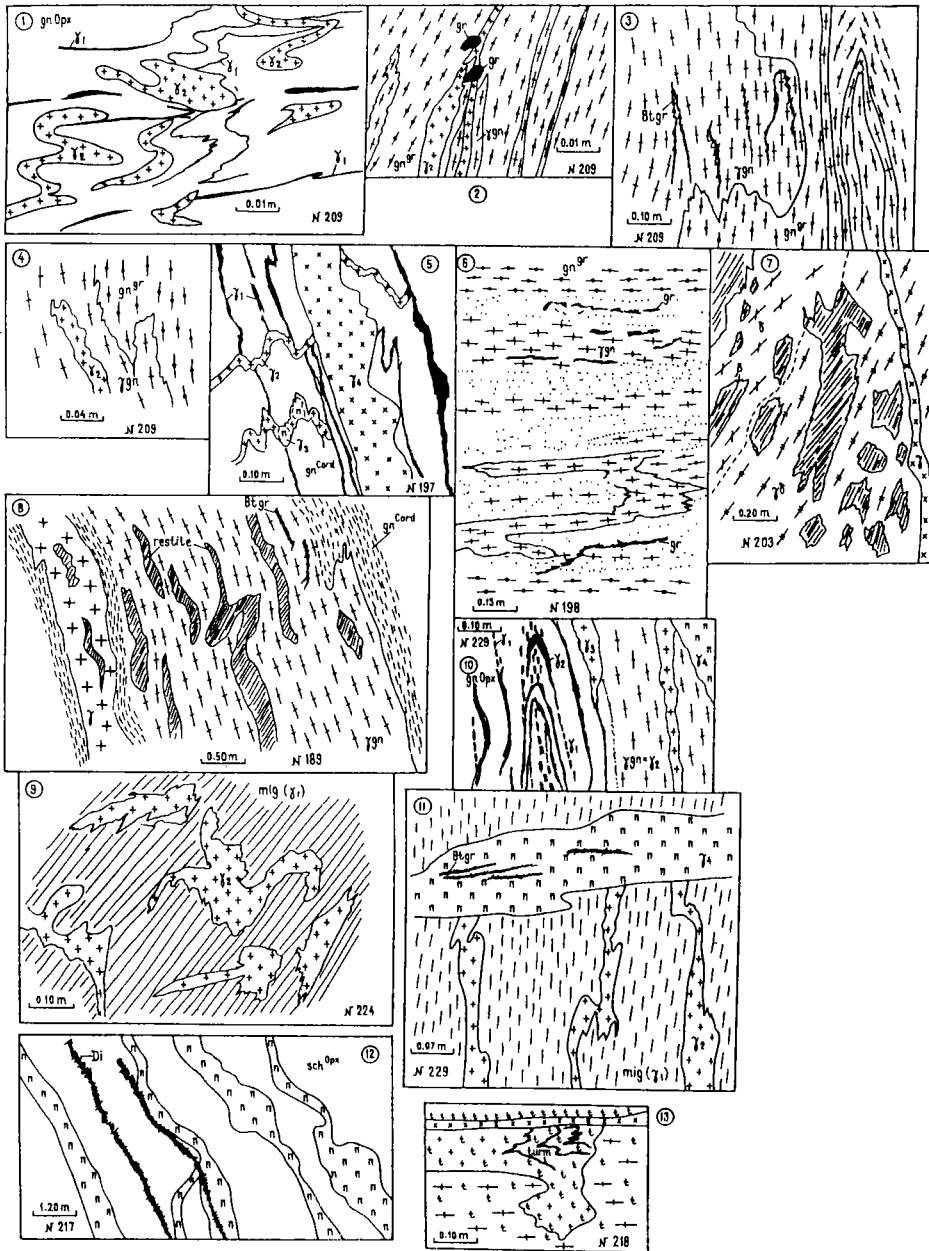


Fig. 4. Relations of the migmatitic leucosome generations and granites in granulite complexes of Northern Korea. Regions: Huichon (1-4, 7), Kanggye (5, 6, 8), Nampo (10, 11), Anju (9), Kimchaek (12, 13). $\gamma_1, \gamma_2, \gamma_3, \gamma_4$: successive migmatitic leucosome generations and pegmatite veins (n) in separate outcrops; gn^{gr}: granite-gneisses (nebulites), mig(γ_1): stromatic migmatites with leucosome of the first generation. Veins and patches (zones of redeposition) of garnet (Gr), biotite (Bt), biotite and garnet (Btgr), K-feldspar (KFsp), quartz (Qtz) and clinopyroxene (Di). Paleosomes are presented by their compositions: gneisses with basic schists (gn^{Opz}), garnet-cordierite and garnet-biotite gneisses (gn^{cord} and gn^{gr}), basic schists (sch^{Opz}). Gneiss remnants among granite-gneisses are denoted by dots, and those with cordierite and biotite are given by hatched area. Relation of tourmaline-bearing plagioclase gneisses (t) and aplite veins (X) with tourmaline veins (turm) is shown in 13. 7 shows intrusive syenite-diorite (δ) and granodiorite ($\gamma\delta$) complex with inclusions of basic rocks (β) and aplite dykes (γ) younger than the Haechon granulites.

magmatic chamber occurring as autochthonous granites, to formation of para-autochthonous and allochthonous granitoid bodies resulting from crystallization of melts uplifted from these chambers.

In the Nangnim complex rather homogeneous, sometimes gneissose and banded granites (usually garnet- and cordierite-bearing) occur. They are identical to granites of the first group [γ_1] according to Korean geologists' data. These granites can be considered as a kind of granite-gneiss with massive structure. They are crosscut by bodies of the coarse-grained (sometimes porphyroblastic) granites [γ_2] and then equilgranular ones [γ_3].

In the Anju region garnet-cordierite-biotite and garnet-biotite gneisses with hypersthene-bearing rock layers contain at least two leucosome generations; the earlier ones form stromatic migmatites, and the later ones (network or stromatic migmatites) occur along the cross-cutting zones and the axial planes of isoclinal folds (Fig. 4-9). Acidleached zones, resulting in quartz-garnet-cordierite and quartz-sillimanite rocks, are overprinted on these migmatites. The granitization of these rocks as well as some leucosomes is characteristic.

The Kimchaek metamorphic complex, developed in the eastern part of the Macheonryong block, gives a Rb-Sr age of 1.71 Ga (Gorokhov *et al.*, 1993). This complex differs from the Nangnim complex by the presence of thick units of marbles, calciphyres and significant amounts of the garnet-free basic schists and quartzites, but by the small amount of aluminous gneisses. The degree of ultrametamorphism in the Kimchaek complex is less intense than that of the Nangnim complex. Moreover, series of subparallel veins of alaskites and pegmatites are widespread (Fig. 4-12). They are intersected by one of the generations of the diopside-phlogopite skarn veins on the Pkhusu deposit. The amount of the leucosomes does not exceed 5–10 vol. %, and their compositions are not granitic and heterogeneous: Pl+Opx (Cpx) or Kfsp+Qz+Pl. In the Pkhusu region tourma-

line-bearing trondhjemite-gneisses, sometimes with hypersthene, occur. They replace quartzites (Fig. 4-13).

More than three generations of the migmatite leucosomes develop in biotite-garnet gneisses, sometimes with sillimanite; the first generation, aligned along banding and schistosity, is very thin and discontinuous, deformed by isoclinal folds, F_1 , and preserved only as ragged relics; the second one is usually thicker and co-planar with the axial surfaces of the F_2 folds; and finally the third one occurs along the cross-cutting zone. Stromatic and network migmatites formed as a result of these events. Crystallization of garnet with increasing granularity in migmatites, formation of selvages consisting of garnet-biotite aggregates, and formation of quartz zone in leucosomes proceeded simultaneously with the above-mentioned events.

The Wonsan granulites consist of garnet-biotite and garnet-cordierite-biotite gneisses, assemblages of which define the garnet-cordierite-biotite-orthoclase subfacies. Biotite and sillimanite are secondary. The univariant equilibrium curve forming biotite + sillimanite has a positive slope in the P-T diagram. Therefore this retrogression can take place either with decreasing temperature or with increasing pressure. Because rather ferrian garnet is generally characteristic, the Wonsan granulite formed at relatively shallow depth.

The early leucosomes, less than 20 vol. %, produce lit-par-lit vein series (up to 1–2 cm thick). Nebulitic migmatites and granite-gneisses form if the amount of leucosome increases to 80–90 vol. %. Coarser-grained granites, including porphyroblastic K-feldspar granites as well as pegmatites, cut early migmatites. Newly formed schistosity and recrystallized zones containing muscovite, biotite, epidote and albite overprint all of these granites.

The granites of other southern exposures (Nampo and Haeju) are preserved rather well among amphibolite facies rocks of the kyanite-sillimanite facies series. They are similar to the Wonsan granulites. Rather ferrian garnet occurs

in aluminous rocks, and a typical assemblage for mafic rocks is two pyroxenes (Opx+Cpx) and An-rich plagioclase in the absence of garnet. The highest-temperature paragenesis Gr+Cord+Opx+Kfsp+Pl+Qz is preserved in the Nampo granulite, consisting mainly of high-Al gneiss. The assemblages of Gr+Bt+Cord+Kfsp+Pl+Qz and Gr+Opx+Bt+Kfsp+Qz+Pl defining moderate temperature subsfacies of the granulite facies are most widespread. In connection with subsequent schistosity formation, the low-temperature assemblages of the garnet-sillimanite-biotite-orthoclase subsfacies overprint the granulite facies migmatites arranged along the isoclinally folded unit boundaries, which were cross-cut by a series of thick veins containing garnet and cordierite (Fig. 4-10). Diffuse veins and irregular bodies of fine-grained granitoid are commonly observed within migmatites. They penetrate all of the other rocks primarily with diffuse contacts, but sharply in some exceptional cases. These relationships result from local melting, subsequent removal of melt, and the generation of network migmatite. The later pegmatoid granite veins transect all of the above mentioned leucosome generations (Fig. 4-10 and 11), and the processes of acid leaching, accompanied by reprecipitation of biotite, garnet and cordierite in the form of folded zones and patches, take place. All of these rocks, including pegmatoid veins, were subjected to schistosity formation resulting in muscovite- or biotite-bearing assemblages that replace hypersthene, garnet, cordierite, and hornblende. Some veins of medium-grained granites and pegmatites occur together with this retrograde metamorphism. Hence, granulite facies rocks are reworked and the amphibolite facies rocks, which are widespread to the north of Nampo, occur. Biotite and biotite-hornblende gneisses, amphibolites and hornblende-plagioclase schists with rare layers of the kyanite gneiss predominate.

CHEMICAL COMPOSITION OF GRANITOID

Table 1. Some average parameters for granite-gneisses and migmatite leucosome 1 of two regions

Regions	n	SiO ₂	MgO	CaO
Kanggye	15	71.6(68.6-76.3)	1.1(0.41-2.98)	1.14(0.5 -2.51)
Huichon	10	68.9(65.4-72.4)	1.6(1.0 -2.36)	2.20(1.08-4.25)

Migmatite leucosomes and granite-gneisses are heterogeneous in composition even within individual granulite block. This heterogeneity results mainly from the variation in the parent rock composition, and less importantly from P-T conditions and ultrametamorphic process character (Sedova and Glebovitsky, 1984; Sedova, 1990). The early leucosomes γ_1 within aluminous gneisses containing pyroxene-bearing rocks (the Huichon region) have higher Ca and Mg, and lower Si contents than those in aluminous gneisses with layering of quartzite-gneisses (the Kanggye region) (Table 1).

For example, in the Kanggye region studied most extensively we trace the evolution of chemical composition of the granitoid. The early migmatite leucosomes, accumulation of which resulted in formation of granite-gneiss, are two kinds: garnet and cordierite varieties. They are oversaturated with Al and Si (mostly 70–75 wt % SiO₂), and are characterized by low CaO and MgO contents (Table 1) and highly variable K₂O (1–6 wt % with a median at 3–4 wt %). The cross-cutting leucosomes and in situ, small granitic bodies [γ_2] within granite-gneiss have similar compositions, but higher K₂O (2–7 wt % with a median at 4–5 wt%) and lower MgO contents. The equigranular, larger granite bodies [γ_1] and [γ_2] containing prophyroblasts of K-feldspar are variable in their compositions. This is due to changing relationship of SiO₂ and K₂O. K₂O always exceeds Na₂O. In contrast to [γ_1] and [γ_2], [γ_3] is more homogeneous and similar to [γ_2] but have higher Na₂O and CaO, and lower K₂O. The frequency maxima of Na₂O, CaO and K₂O for [γ_3] are 4-5, 1-2 and 3-4%, respectively, in contrast to those (2-3, 0-1 and 4-5) for [γ_2].

These specific features are already displayed

a small slope, indicating the F_2 increase with intensification of processes related to K-feldspar formation in some granitoid types (Fig. 5a). The variations of F_3 are significant as well, which witnesses heterogeneity of some leucosome veins and their differentiation during and after the formation of melts from partial fusion of granite-gneisses and migmatites. Three data for γ_3 fall within γ_2 field.

The fields for $[\gamma_1]$, $[\gamma_2]$ and $[\gamma_3]$ do not indicate that they formed from differentiation of a single magma. $[\gamma_1]$ and $[\gamma_2]$ have lower acidity and higher maficity relative to γ_1 and partly γ_2 . The parent melt for them seems to have been derived from significantly deeper level. In contrast to them $[\gamma_3]$ has reverse relationship with γ_1 and γ_2 in acidity, maficity and alkalinity, and might be mobilized from γ_1 , like γ_2 , but are mature and therefore homogenous. $[\gamma_1]$ and $[\gamma_2]$, belonging to different massifs, reflect different degrees of albitization and K-feldspathization. Therefore increase in Na activity at constant K is characteristic for $[\gamma_1]$, and increase in Na and K activity takes place in equal degree for $[\gamma_2]$.

THERMO- AND BAROMETRIC METHODS

There exist several tens of mineralogical thermometers and barometers, based on the law of equilibrium element distribution between mineral phases. The most efficient thermometers were calibrated by calculating the thermodynamic effect of isomorphic species distribution between solid phases for cation-exchange reactions of the following type :



where α_{Mg} , β_{Mg} , α_{Fe} , and β_{Fe} are Mg and Fe components of α and β minerals, respectively.

An equilibrium in the reaction is described by the equation :

$$RT \ln K_D = \Delta G_T = \Delta H^\circ_T - \Delta S^\circ_T + P \Delta V \quad (2)$$

where K_D , defined by $\{X_{Mg,\beta} (1 - X_{Mg,\alpha})\} / \{X_{Mg,\alpha} (1 - X_{Mg,\beta})\}$, is the Mg and Fe distribution coefficient between phases α and β , X_i is the mole fraction of the i th species (Mg or Fe) in the phase, T is temperature in K, R is the universal gas constant, ΔG_T is the change in the Gibbs free energy, ΔH°_T is enthalpy, and ΔS°_T is entropy of the cation-exchange reaction, ΔV is volume change of the reaction, and P is pressure. Because ΔV is insignificant, K_D is nearly independent of pressure, and most cation-exchange equilibria are fairly good thermometers.

There exist two factors complicating the thermometric work. Many researchers experimentally and theoretically demonstrated that activities of the isomorphic species (Fe and Mg in this case) depend on the concentration of other species, for example, on Ti and Al contents of biotite, and Mn and Ca of garnet. Thus, the increase of Ti or Al in biotite increases the Mg activity, and it migrates into a co-existing phase and changes the K_D value, as well as the measured temperature.

Another complicating factor is the deviation from ideal Fe and Mg distribution. K_D depends not only on temperature and the concentration of other species, but also on the degree of isomorphic replacement.

Garnet-biotite thermometer is commonly used for solving metamorphic petrology problems. There are more than 20 versions of this thermometer. Twenty years ago we (Glebovitsky *et al.*, 1972) inferred the relationship between K_{Mg}^{Gr-Bt} and temperature for the $Gr + Cord + Bt + Ort + Pl + Qz$ assemblage which is stable in a wide range of temperature and pressure. Our equation is as follows :

$$1000/T \text{ (K)} = 0.334 \ln K_D + 0.154 X_{Mg}^{Gr} + 0.539 \quad (3)$$

where $K_D = \{X_{Mg}/(1 - X_{Mg})\}^{Bt} / \{(1 - X_{Mg})/X_{Mg}\}^{Gr}$, and $X_{Mg}^{Gr} = Mg/Mg + Fe + Mn + Ca$. In this case only the Mg content of garnet and its influence on K_D were taken into account. For the same assemblage, the equation for pressure is :

$$P \text{ (kb)} = 25.81 + 2.26 \ln \left[\frac{\text{Si}^{\text{Bt}} \text{Al}^{\text{BtVI}} / \text{Al}^{\text{BtIV}} (\text{Ti} + \text{Fe} + \text{Ca} + \text{Mn})^{\text{Bt}}}{\text{Mg} / \text{Mg} + \text{Fe} + \text{Ca} + \text{Mn}} \right]^{\text{Gr}} - 11.83 \text{Al}^{\text{Bt}_{\text{tot}}}, \quad (4)$$

where Si^{Bt} , Al^{BtVI} , Al^{BtIV} , $\text{Al}^{\text{Bt}_{\text{tot}}}$, and Ti^{Bt} are the atomic contents of Si, octahedral, tetrahedral and total Al, and Ti in biotite. Note that pressure determination is based on the well-known effect of Al-distribution between octahedral and tetrahedral sites in biotite, and the Mg content in garnet increasing in the above assemblage with increasing P and decreasing T. To be absolutely exact, pressure calculated from (4) should take into account the effect of temperature, although this effect is negligible. For certain pressure determination, the Al content of biotite must be precisely measured, and high quality of chemical analyses is necessary.

In (3) the effects of Ca, Mn and Fe in garnet, and Fe in biotite on the K_D value were not taken into account. Thus, this thermometer based on (3) does not always give satisfactory results. Therefore Glebovitsky and Drugova (1979) re-examined the garnet-biotite thermometer. Firstly, the relationship between temperature and K_D for ideal Fe-Mg distribution was inferred using (2):

$$T(^{\circ}\text{C}) = 1250 K_D + 385 \quad (5)$$

Then the following formulas relating the K_D value to concentrations of the above mentioned elements were obtained: for staurolite schists,

$$\Delta K_D = 0.41(\text{Fe}^{\text{Gr}} - 2.41) + 0.38(\text{Mn}^{\text{Gr}} - 0.20) + 0.37(\text{Ca}^{\text{Gr}} - 0.31) - 0.19(\text{Fe}^{\text{Bt}} - 1.10); \quad (6)$$

for gneisses of high-rank amphibolite facies,

$$\Delta K_D = 0.43(\text{Fe}^{\text{Gr}} - 2.12) + 0.25(\text{Mn}^{\text{Gr}} - 0.10) + 0.23(\text{Ca}^{\text{Gr}} - 0.29) - 0.38(\text{Fe}^{\text{Bt}} - 1.06); \quad (7)$$

for gneisses of the granulite facies,

$$\Delta K_D = 0.30(\text{Fe}^{\text{Gr}} - 1.80) + 0.97(\text{Mn}^{\text{Gr}} - 0.03) + 0.25(\text{Ca}^{\text{Gr}} - 0.20) - 0.38(\text{Fe}^{\text{Bt}} - 0.82). \quad (8)$$

It has been already pointed out that (3), (6), (7)

and (8) do not take into account the effect of other components in biotite. The most important variables are the Ti content and the Al distribution between octahedral and tetrahedral sites of biotite.

Other attempts to calibrate the Bt-Gr thermometer led to the similar result. Perchuk *et al.* (1985) obtained the following equation which includes the pressure term:

$$T(^{\circ}\text{C}) = (7842 + 25P) / (5.699 + 1.987 K_D^{\text{Bt-Gr}}) - 273 \quad (9)$$

where $K_D^{\text{Bt-Gr}} = \left[\frac{X_{\text{Mg}}}{1 - X_{\text{Mg}}} \right]^{\text{Bt}} / \left\{ \frac{(1 - X_{\text{Mg}})}{X_{\text{Mg}}} \right\}^{\text{Gr}}$, $X_{\text{Mg}} = \text{Mg} / \text{Mg} + \text{Fe} + \text{Mn}$, and P is pressure in bars. This thermometer was improved by Aronovich (1988) in order to take into account Ca effect in garnet ($X_{\text{Ca}}^{\text{Gr}} = \text{Ca} / \text{Ca} + \text{Mg} + \text{Fe} + \text{Mn}$):

$$T(^{\circ}\text{C}) = (7843 + 25P) / (5.699 + 1.9871 \ln K_D - 1.242 X_{\text{Ca}}^{\text{Gr}}) - 273 \quad (10)$$

In this paper we demonstrate that these equations give results consistent with those calculated from (3). However, obviously low temperatures are often measured: for example, temperatures significantly below 700°C for hypersthene-garnet gneisses necessitate corrections for using (6)–(8).

Similar results are apparent for the garnet-cordierite thermometer.

$$T(^{\circ}\text{C}) = (6134 + 35P) / (2.688 + 1.9871 \ln K_D^{\text{Card-Gr}}) - 273 \quad (11)$$

and the garnet-staurolite thermometer

$$T(^{\circ}\text{C}) = 5391 / (5.561 + 1.9871 \ln K_D^{\text{St-Gr}}) - 273 \quad (12)$$

(Perchuk, 1989). The common drawback for all of these thermometers is the lack of information on the dependence of K_D on Ti and Al contents in biotite. Their effect might be estimated for the orthopyroxene-biotite thermometer by the equation (Sengupta *et al.*, 1990):

$$T(^{\circ}\text{C}) = 4130 - 630(X_{\text{Mg}} - X_{\text{Fe}})^{\text{Opx}} - 4423 X_{\text{Ti}}^{\text{Bt}} - 3395 \text{Al}_{\text{VI}}^{\text{Bt}} + 0.017 P / 1.98 K_D^{\text{Bt-Opx}} - 3.27 \quad (13)$$

where $X_{\text{Ti}}^{\text{Bt}} = \text{Ti} / \text{Fe} + \text{Mg} + \text{Al}_{\text{VI}} + \text{Ti}$, $\text{Al}_{\text{VI}}^{\text{Bt}} = \text{Al}_{\text{VI}} /$

Table 3. Granulite facies metamorphic conditions in the Nangnim block

Sample No.	Rock types	Mineral assemblages	TBG	PBG	P	A	B	TGC	TGO	TOB
Kanggye region										
189-16	c-m	nebulite	Bt + Gr + Cord + KFsp + Pl + Qtz	811	5.5					
		granite-gneiss	(secondary Sil)	683	6.0					
189-12	c-r	nebulite mobilized (perhaps γ_2)	Bt + Gr + Cord + KFsp + Pl + Qtz	760	4.8					
	r-r			725	4.9					
190-10	c-m	Gr. of cross-cutting body ($\gamma_{3,4}$)	Bt + Gr + KFsp + Pl + Qtz	673	5.9					
	r-r			667	5.5					
190-11	c-m	Restite in granite (190-10)	Bt + Gr + Cord + KFsp + Pl + Qtz	718	5.3					
	r-r			535	3.4					
194-1	c-r	Gr. (γ_1)	same	712	7.2					
	r-r			670	6.9					
195-1	c-m	Gr. (γ_2)	same	766	6.8					
197-8	c-m	Gr. dyke (γ_4)	same	728	7.2					
	r-r			721	6.7					
Huichon region										
207-1p	c-m	Secondary sheared paleosome	Bt + Gr + Opx + KFsp + Pl + Qtz	781	7.6	7	704			
	r-r			750	6.8	7	640			
207-11	c-m	Secondary sheared leucosome	same	751	7.0					
	r-r			734	7.6					
208-6	c-m	Mig. schist	same	635(678)	3.7	4			625	
	c-inc		Qtz less than 5%	696(730)	4.9					
	r-r			649(680)	5.6					
209-1	c-inc	Mig. gneiss	same	775	4.0	4	701			
	c-inc			748	4.2	4	690			
	c-m			842	5.1	5	760			
	c-m			750	6.1	6	650	670	643	
	r-r			715	6.7	7	608			
209-2p	c-m	Paleosome of migmatite generation 1, 2	Bt + Gr + Opx + Pl + Qtz	813	6.1	7	774	741	811	
	r-r			773	6.8	7	717			
	r-r			749	6.2					
209-21	c-m	Leucosome	Bt + Gr + Opx + KFsp + Pl + Qtz	714	7.4	7	670			
	r-r			730	6.9	7	570			
209-10	c-r	Secd. sheared migmatite	same	755	5.9	6	664			
	r-r			733	6.3	6	578			
Anju region										
139-1		Mig. gneiss	Bt + Gr + Opx + KFsp + Pl + Qtz	768(790)	7.6	7	692		717	739
139-3		same		754(780)	7.5	7	637		649	722
91-1		same	same	729(750)	4.6	5	649		721	716
224-3		Leucosome of net work migmatite ($\gamma_{3,4}$)	Bt + Gr + Cord + Kfsp + Pl + Qtz	774	5.5					
				749	6.0					
88-4		Leucosome of net-work migmatite	same	746	6.0	6	680			
88-3		Gneiss	same	720	6.5					
137-1		Gneiss	same	658(740)	6.2	6	643		780	
137-2				675(690)	6.3	6	659		727	
137-3				639(650)	5.9	6	576		640	
69		Gneiss	Bt + Gr + KFsp + Pl + Qtz	779	4.9	5	770			
				668	5.2	5	570			
53-4		Gneiss	Bt + Gr + Cord + KFsp + Pl + Qtz	775	6.2					
53-2				825	5.5					
53-1				780	5.9					
53-1				764	5.6					

Symbols : c-m, garnet core and matrix biotite; r-r, garnet rim and biotite in contact with garnet; c-r, garnet core and biotite in contact with garnet; c-inc, garnet core and biotite inclusion. If no comments are given, any mineral compositions are listed. All pressures and temperatures were calculated assuming total Fe as Fe^{2+} . T_{Gd}^{Bt-Gr} (TBG) and P_{Gd}^{Bt-Gr} (PBG) were calculated using equations (5-8) and (4) of the present work (Glebovitsky and Sedova, 1979). T in brackets are corrected for the Ca content in garnet. $T_P^{Bt-Gr}(A)$, $T_P^{Bt-Sil}(TBS)$, $T_A^{Gr-Cord}(TGC)$, $T_{LP}^{Gr-Opx}(TGO)$ and $T_S^{Opx-Bt}(TOB)$ were computed from equations 10, 11, 13, 14 of this work (Perchuk *et al.*, 1985; Aranovich, 1988; Lavrentyeva and Perchuk, 1990; Sengupta *et al.*, 1990). P- pressure accepted for temperature calculations. *-without correction for the Mn content of garnet. T : °C and P : kb.

Mg+Fe+Al_{v1}+Ti, and P is pressure (in bars). Both X_{Ti} and Al_{v1} values significantly reduce the calculated temperature.

The distribution of Fe and Mg within mineral pairs involving orthopyroxene significantly depends on the Al content of orthopyroxene (Lavrentyeva and Perchuk, 1990). The Opx-Gr thermometer of Lavrentyeva and Perchuk (1990) was used in this study :

$$\begin{aligned} T(^{\circ}\text{C}) = & 4066 - 347(X_{\text{Mg}} - X_{\text{Fe}})^{\text{Opx}} - 171184 X_{\text{Al}}^{\text{Opx}} \\ & - 5769 X_{\text{Ca}}^{\text{Gr}} + 23.42P / (1.9871 \ln K_D) \\ & + 2.143 + 0.0929(X_{\text{Mg}} - X_{\text{Fe}})^{\text{Opx}} 12.894 X_{\text{Al}}^{\text{Opx}} \\ & + 5.846 X_{\text{Ca}}^{\text{Gr}} - 273 \end{aligned} \quad (14)$$

where $K_D = (X_{\text{Mg}}/1 - X_{\text{Mg}})^{\text{Opx}}(1 - X_{\text{Mg}}/X_{\text{Mg}})^{\text{Gr}}$, $X_{\text{Mg}} = \text{Mg}/\text{Mg} + \text{Fe} + \text{Mn}$, $X_{\text{Ca}}^{\text{Gr}} = \text{Ca}/\text{Ca} + \text{Mg} + \text{Fe} + \text{Mn}$, and $X_{\text{Al}}^{\text{Opx}} = \text{Al}/2(\text{Mg} + \text{Fe} + \text{Mn} + 0.5\text{Al})$.

To estimate metamorphic pressure, we used some new geobarometers. For the equilibrium $\text{Gr} + \text{Mus} = \text{Qz} + \text{Sil}(\text{Ky}) + \text{Bt}$, the following barometer was proposed by Perchuck *et al.* (1985) :

$$\begin{aligned} P(\text{kb}) = & (10066 + T(\text{K})(-1.948 - 1.9871 \ln K \\ & + 6432 X_{\text{Ca}}^{\text{Gr}}) / 437 \end{aligned} \quad (15)$$

where $K = X_{\text{Mg}}^{\text{Bt}}/X_{\text{Mg}}^{\text{Gr}}$, $X_{\text{Mg}} = \text{Mg}/\text{Mg} + \text{Fe} + \text{Mn}$, $X_{\text{Ca}}^{\text{Gr}} = \text{Ca}/\text{Ca} + \text{Mg} + \text{Fe} + \text{Mn}$; and for the equilibrium $\text{Gr} + \text{Sil} + \text{Qz} = \text{Cord}$:

$$\begin{aligned} P(\text{kb}) = & (6 + G^{\text{e}}_{\text{Cord}}/2 - (T + 273)(4.598 + 1.9871 \\ & \ln K)) / (-V^{\text{e}}_{\text{Cord}} - 638.3) \end{aligned} \quad (16)$$

where $K = X_{\text{Mg}}^{\text{Cord}}/X_{\text{Mg}}^{\text{Gr}}$, $G^{\text{e}}_{\text{Cord}} = -1333 + 0.617T(\text{K}) + 1026(1 - H) + 472(1 - H)^2$, $V^{\text{e}}_{\text{Cord}} = -336$, and $H = \text{H}_2\text{O}/\text{H}_2\text{O} + \text{CO}_2$ in fluid.

During this study some mineral equilibria were calculated using available thermodynamic data in order to provide P and T constraints for thermobarometric determinations. In some fluid inclusions of samples whole mineral compositions of mineral were determined, H₂O-rich solution and pure CO₂ inclusions were found and investigated by Vapnik. Pressure was also estimated from the study of fluid inclusions.

P-T CONDITIONS AND P-T-TIME PATHS OF EVOLUTION

The P-T conditions of each metamorphic complex are described below.

Nangnim block

In nebulites (γ_1) of the Kanggye region, formed simultaneously with granulite metamorphic peak were estimated as 811°C and 5.5 kb for the assemblage $\text{Gr} + \text{Cord} + \text{Bt} + \text{Kfsp} + \text{Pl} + \text{Qz}$ (189-16, Table 3). The compositions of garnet core and biotite from the fine-grained matrix were used. The P-T values using garnet rim together with biotite in contact with garnet suggest a significant cooling down to 683°C at the pressure of 6 kb. During this cooling, the acid leaching formed quartz-sillimanite metasomatic rock both in leucosome and melanosome (or restite) of the nebulites. Parautochthonous, insignificantly removed granites (γ_2) indicate the temperature of 760–727°C at low pressure of 4.8–4.9 kb. In later homogeneous granites cross-cutting other rock bodies (γ_3), temperature decreases to 670°C (190–10) at 5.5–5.9 kb, and pressure to 3.4 kb only after cooling to 535°C. It should be pointed out that cordierite-garnet-biotite granites, showing ordinary temperature of the granulite facies (197-8), intruded only after significant cooling and decompression. However, these granites occur in the region far from those considered above.

Interesting data concerning the large massif of homogeneous porphyritic granite [γ_2] (194-1 and 195-1) were obtained. At 710–730°C, pressure reaches 7.2 kb, corresponding to the depth of onset of magma crystallization. In this case the pressure of 5.5–5.9 kb measured in the country gneisses (190–10) was preserved during cooling to 670°C. This P-T condition represents the final stage of magma crystallization and formation of the granite massif. Thus, in the Kanggye region, nearly isobaric cooling by greater than 100°C after the peak metamorphism is established (Fig. 6).

Table 4. Granulite facies metamorphic conditions in the Chungsan belt

Sample No.	Rock types	Mineral assemblages	TBG	PBG	P	A	TGC	TGO	TOB	P _p	
Nampo region											
49-2	c-inc	Mig. Gn.	Bt + Gr + Cord + Kf + Pl + Qz		776	7.4	7	526			
	c-inc		*sil		764	6.7	7	526			
	r-r				742	7.2	7	649	656	6.1	
	r-r				770	8.2	8	590	573	5.3	
	r-r				728	6.8	7	622			
45-4	c-m	Gn.	Bt + Gr + Sp + Sil + Pl + Qz		923	5.9	6	864			
48-4	c-m	Mig. Gn.	Bt + Gr + Cord + Kf + Pl + Qz		777	6.3	6	760			
	r-r				700	5.3	5	691			
47-1	r-r	Gn.	Bt + Gr + Sil* + Mu* + Qz		670	5.3	5	662			
143-4b		Mig. Gn.	Bt + Gr + Pl* + Qz		778	5.9	6	726			
143-2b		same	Bt + Gr + Cord + Opx + Kf + Pl + Qz		859	6.9	7	755	777	672	848
149-3a					841	7.2	7	687	699	706	
149-3a		same	Bt + Gr + Opx + Kf + Pl + Qz		769	4.9	5	678	707		690
149-3b					793	6.2		722	707	698	784
143-6		same	Bt + Gr + Cord + Sil* + Kf + Pl + Qz		814	6.7	7	766	780	6.3	
					775	6.3		669	689		
143-8		same	same		804	5.7	6	780	846	6.2	
175-1	c-m	Mig. Gn.	same		754	6.6	7	680		7.5	
	r-r				740	6.5	7	670		7.5	
175-4		Leuc.	same		716	5	5	561	670	5.2	
94-1	c-m	Mig. Gn.	Bt + Gr + Cord + Kf + Pl + Qz		800	7					
	r-r				749	6.8					
Haeju region											
3-3	c-m	same	Bt + Gr + Sil + Kf + Pl + Qz		782	6	817				
	r-r				735	6.5	6	629			
76-7	c-m	same	Bt + Gr + Cord + Sil + Kf + Pl + Qz		779	5.3	5	760	767	6	
	r-r				740	5.8	6	727	704	6.5	
76-9	c-m	same	same		775	5.2		730	784		
77-4		same	Bt + Gr + Cord + Sil + Pl + Qz		698	6.1	6	638			
					645	6.3	6	585			
					681	6.2	6	676			
					663	6.5	6	616			
					685	6.2	6	616			
					663	6.5	6	616			
3-5		same	Bt + Gr + Cord + Kf + Plz		815	5.1					
		same	same		768	5.1					
Wonsan region											
186-3	c-m	Pale.	Bt + Gr + Cord + Kf + Pl + Qz		808	5.1					
	r-r	Mig.			778	4.9					
186-3	c-m	Leuc.	same		759	5.8					
	r-r				645	5.2					
186-4	c-m	Mig./w	same		791	5.2					
	r-r	Leuc.			725	5.4					
186-6	c-m	Mig./w	same		769	5.2					
	r-r	Leuc.			773	5					

All symbols are same as in Table 3. P_p is pressure calculated according to equations 15 and 16 (Perchuk *et al.*, 1985). *-secondary minerals.

equilibria between garnet rims and in contact biotite from migmatite mesosomes (209-2 m, r-r), migmatite leucosomes (209-21), the shear zones overprinting all generations of migmatite (207-1 and 209-10) indicate pressures greater than 6 kb, reaching 7.6 kb at 714–780°C. Hence, in the Hui-chon granulites, a cooling path with increasing pressure is distinct. Furthermore, the low pressure episode has occurred at moderately high temperature before the metamorphic culmination (Fig. 6).

Geological and analytical data for the Anju region allow us only a general description of P-T conditions and their evolution. For hypersthene-bearing gneisses (139-1 and 139-3, Table 3) temperatures are 754°C and 765°C at 7.5 and 7.8 kb. These data are consistent, but unreliable because biotite is enriched in Al and low in Si. Temperatures determined by garnet-orthopyroxene and orthopyroxene-biotite thermometers are compatible with those of the Gr-Bt thermometer. However, the latter estimates based on (10) are significantly lower. The garnet-cordierite granites retrograded at similar temperature, but at lower pressure (5.5–6.5 kb, 224-3, 88-4 and 88-3). The P estimate is more reliable because the biotite-garnet thermobarometer used here is primarily calibrated for the cordierite-bearing paragenesis (Glebovitsky and Drugova, 1979). Other samples of garnet-biotite-cordierite gneisses (137-1, 137-2, and 137-3) significantly vary in temperature estimated from (10). Temperatures of the garnet-biotite thermometer are significantly lower than those the garnet-orthopyroxene and orthopyroxene-biotite thermometers. Because these gneisses alternate with orthopyroxene schists, corrections are made using (8) to produce temperatures close to those of the garnet-cordierite and biotite-orthopyroxene thermometers for 139. The sequence 69 → 224-3 → 88-4 → 88-3 → 137 may define the cooling path with increasing pressure (Fig. 6). Further retrograde metamorphism may occur under the amphibolite facies condition observed at the southern margin of the Nangnim

block. This suggestion is supported by two P-T measurements in sample 87; 668°C, 5.2 kb and 617°C, 3.5 kb.

The data reported above for the Nangnim block lead to the following conclusions;

1. The earliest metamorphic event characterized by temperature of the granulite facies (740–750°C) and by moderate pressure (4–5 kb) define a high geothermal gradient.
2. Peak metamorphism occurred at 800°C and 5.5–6 kb, and accompanied anatexis, granitization and migmatite formation. The parent magma for [γ_2] was generated at a depth greater than that of peak metamorphism.
3. Further evolution proceeded with the crystallization of anatectic magma forming small bodies of granite and pegmatite. During this process, the cooling occurred either isobarically or with increasing pressure.
4. The P-T-time path shows an anticlockwise pattern.

The Chungsan belt

Assemblages of the granulite facies corresponding to the earliest metamorphic episode are well preserved within Chungsan belt. In the Wonsan region gneisses containing Gr+Cord+Bt+Kfsp+Pl+Qz are widespread. Equilibrium temperatures between garnet and biotite, were calculated using (5), (7) and (8). As described below, these temperatures are in good agreement with the Perchuk's (1985) thermometer, although the latter is systematically lower by 50–70°C. The pressure determined by the Gr-Cord-Sil barometer is usually greater than that of (4), because in the former the activity of H₂O is assumed to be equal to one. This pressure corresponds to the cooling stage, because sillimanite with secondary biotite occurs by retrograde alteration with increasing $\alpha_{\text{H}_2\text{O}}$ of fluid. All of the P-T measurements indicate a cooling at constant pressure, together with the peak metamorphic condition corresponding to 800°C and 5.5 kb (Ta-

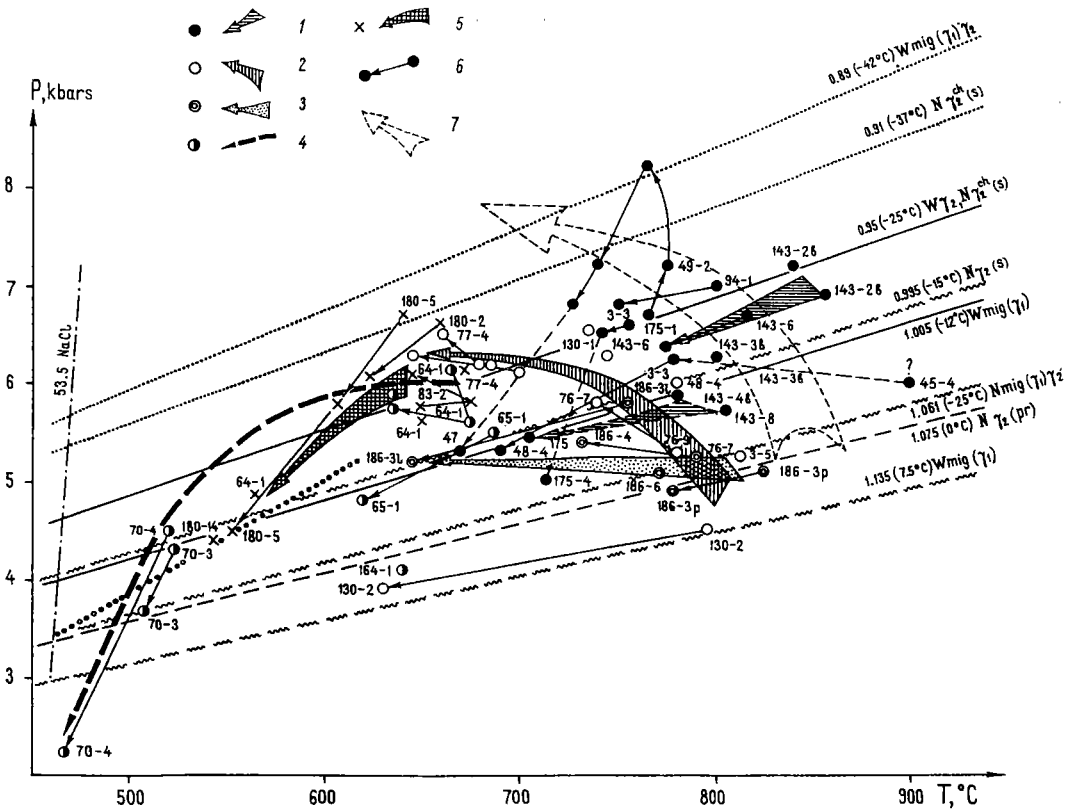


Fig. 7. Metamorphic conditions and P-T-time evolution paths of the granulite and amphibolite facies rocks of the Chungsan belt. Data for each sample and general trends are shown for the following regions: Nampo (1), Haeju (2), Wonsan (3), Kwail (4), Chungsan (5). Separate trends for individual samples (6) and a hypothetical trend for the Nampo gneisses (7) are also shown. Question mark near point 45-4 indicates the uncertainty because of high Mg content of garnet. Symbols of CO₂ isochores and rock group of different regions are given in Fig. 9. The CO₂ isochore for primary inclusions (pr) in migmatite leucosome of the second generation (γ_2) in the Nampo region is shown by heavy dashed line. Liquidus line (dash and point) in the system H₂O–53.5 wt % NaCl adopted from Roedder (1988) corresponds to salt-water inclusion in quartzes of 2 (Wonsan). Isochore with density of 1.1 g/cm³ for a system H₂O–30 wt% NaCl given for salt-water inclusions of sample 180 is displayed according to Touret (1986).

ble 4, Fig. 7).

Cordierite-garnet-biotite \pm sillimanite gneisses of the Nampo region near the Taedong river mouth were studied in detail, and the results are apparently contradictory. From the early to late stages (49-2, c-inc and r-r), temperatures based on (5) and (8) decrease from 770°C to 730°C. Furthermore, pressure initially increases almost isothermally by more than 1 kb, and then decreases with cooling. However, the P calculation for the same sample using (16) together with the Gr-Bt temperature based on (9) gave significantly low

pressure. Biotite of 49-2 is very high in the Mg content, and the non-ideality of Bt solid-solution results in decrease in temperature and pressure. Therefore, for this sequence, temperature and pressure calculated from (4) and (5) were used. It was not possible to determine the peak metamorphic condition because of strong retrogression of garnet and cordierite to biotite and sillimanite. This alteration can be explained by a pressure increase together with slight cooling.

A distinct tendency of retrograde alteration was discovered in a series of samples 45,48 and 47.

Table 5. Conditions of amphibolite facies metamorphism in the Chungsan belt

Samles	Rocks	Mineral assemblages	TBG	PBG	A	TGS	P _p
164-1	c-m Gn.	Bt + Gr + Sil + Ms + Pl + Qz	640	4.1	662		6.4
83-2	c-m same	Bt + Gr + Ms + Pl + Qz	635	5.9	679		
	r-r		573	5.6	679		
	c-m		666	6.1	607		
	r-r		637	5.8	611		
82-3	c-m same	Bt + Gr + Sil + Ms + Pl + Qz	994	5.6	901		
	c-m	Gr inequib.	780	5	817		
70-3	c-m alt. Gn.	Bt + Gr + Chl + Ms + Pl + Qz + Ep	523	4.3	538		
	r-r		508	3.7	575		
70-4	c-m same	same	521	4.5	566		
	r-r		470	2.2	572		
180-2	c-m Gn.	Bt + Gr + St + Ms + Ky + Pl + Qz	579	3.3	660	732	6.6
	r-r		556	4.1	625	640	6
180-5	c-m Gn.	same	583	4.2	608	620	6.7
	c-m		609	4.3	637	662	6.7
	r-r		579	3.7	550	550	4.5
180-14	r-r same	same	578	4.4	543	548	4.3
64-1a	c-m same	Bt + Gr + Ms + Ky + Pl + Qz	635	3.4	647		6
	c-inc		633	3.3	670		5.8
	c-inc		665	3.6	670		5.8
	r-r		655	3.3	671		6.2
	r-r	inequib.assmb.	699	3.8	737		7.4
64-1	same	Bt + Gr + Ms + Ky + Pl + Qz	613	3.4	648		5.6
125-8	same	Bt + Gr + Sil + Ms + Pl + Qz	594	3.6			
131-3	same	same	630	6.3			
131-5	same	same	680	4			
65-1b	same	same	688	5.4	603		
61-5b	alt. Gn.	Bt + Gr + Chl + Sil + Pl + Qz + Ep	620	4.8	641		

In Gr-Bt-Spinel-Sil gneiss (45), garnet is enriched in Mg, and temperatures based on (5), (8), and (10) exceed 900°C. P-T estimates for 48-2 are in good agreement with the onset point of P-T path for 49 (Fig. 7). In the highly-retrograded outcrop of 47, temperatures are 670 and 662°C. These temperatures belong to the stability field of muscovite. Pressure (7.2 kb) estimated by the Gr-Sil-Mus barometer is higher than that calculated by (4) (5.3 kb). In every case it is clear that the cooling was not accompanied by decompression.

The peak metamorphic condition seems to be determined in 143. The P-T estimates of 143-e (777°C and 6.9 kb) and 143-3a (769°C and 4.9 kb) are uncertain because of high Mg content in garnet, and those of the highest temperature paragenesis Gr + Cord + Opx + Kfsp + Pl + Qz (800°C

and 7 kb) are more reliable. Calculations for the sequence 143-3b → 143-4b → 143-6 result in cooling to the beginning of P-T path for 49. The P-T path defined by 94 documents a cooling of 50°C at constant pressure. Samples 175-1 and 175-4 decrease in temperature from 750°C to 710°C at 5.6 kb, and represent the minimum P-T condition for the stability of Cord + Gr + Bt + Sil + Kfsp + Pl + Qtz (Fig. 7).

In the Haeju region garnet-biotite-cordierite gneisses of the granulite facies are widespread. Culmination of metamorphism might be described as 815°C and 5.2 kb for 3-3, 76-7, 76-9 and 3-5 in which Mg-rich garnet occurs. If other analyses for 77-4 (Table 4) are considered, the cooling apparently took place with increasing pressure.

Pressures estimated from the Gr-Sil-Mus and

Table 6. Granulite facies metamorphic conditions in the Macheonryong belt

Samles Rocks	Mineral assemblages	TBG	PBG
219-11 Leuco.	Bt + Gr + Kf + Pl + Qz	761	6.7
Mig.		798	6.8
219-3p Paleo.	same	789	6.5
Mig.		763	7
219-4 same	same	746	6.7
		760	7
219-61 Leuco.	Bt + Gr + Cord + Sil	760	6.3
Mig.	+ Kf + Pl + Qz	774	6.4
219-71 Leuco Mig.	Bt + Gr + Kf + Pl + Qz	756	6.6
8049 same	same	813	7.4
8042 same	same	826	6.6
8716 same	same	805	6.5
		804	6.9

All symbols are same as in Table 3.

Gr-Cord-Sil equilibria are significantly greater than those from (4). The application of the Gr-Sil-Mus barometer is limited to the stability field of muscovite. Moreover, garnet and sillimanite are usually not in equilibrium with muscovite, and represent the higher temperature stage of evolution. On the other hand, the Gr-Cord-Sil barometer depends on the H₂O activity in fluid. Pressure values calculated by different methods practically coincide at X_{H₂O} = 0.4, but differ more significantly with increasing X_{H₂O}.

Data in Table 5 for the Chungsan belt establish the P-T condition of the amphibolite facies metamorphism: T = 650°C and P = 6.0–6.5 kb corresponding to the kyanite-sillimanite facies series of Miyashiro. This P-T condition coincides with that of the retrograde evolution in Nampo and Haeju granulites. Furthermore, P-T data in Table 5 suggest a retrograde path down to 500°C and 4.2 kb (Fig. 7), and then to 470°C and 2.2 kb.

In summary, regional metamorphism of the Chungsan belt evolved from an early granulite facies to the following sequences:

1. The peak metamorphic condition of the Nampo region is 800–900°C and 6–7 kb, and that of the southern exposures and the Wonsan region 800°C and 5 kb.

2. After the culmination, the cooling of meta-

morphic units took place either isobarically or with increasing pressure.

3. The Al-rich gneisses of the granulite facies evolved into the amphibolite facies of the kyanite-sillimanite facies series. Retrograde path may pass through 470°C and 2.2 kb.

The Macheonryong belt

This metamorphic belt belongs to the andalusite-sillimanite type, and can be subdivided into the Sangnong zone of the greenschist to amphibolite facies and the Kimchaek zone where the granulite facies dominate.

Data on metamorphic condition of the Kimchaek zone are extremely limited. Carbonate rocks and two-pyroxene schist are widespread. In the latter, rare garnet appears. In the marginal part of the Kimchaek zone actinolite and Al-poor hornblende occur, and garnet forms after these minerals. The X_{Mg} value of garnet changes from 0.2 to 0.24, suggesting an increase in pressure. Primary minerals include plagioclase of high An content (up to An₉₀) that indicates low pressure.

In the Sariwon apatite deposit region, the later 'eclogitization' is rather common and leads to the formation of garnet-pyroxene (X_{pyroxene} = 0.245 and X_{Mg} = 0.31) and hornblende-garnet (X_{pyroxene} = 0.213, X_{Mg} = 0.27). Temperatures of their formation, estimated from the Gr-Cpx and Gr-Amph thermometers, are 790°C and 690°C, respectively. Moderate alumina Gr-Bt gneisses suggest low P metamorphism in contrast to mafic schists. The calculated pressures range from 6.2 to 7 kb at 750–860°C (Table 6 and Fig. 8). These P-T estimates suggest an isobaric cooling. Samples from the Pkhosu phlogopite deposit give 815–830°C at pressures not less than 7 kb. This result consistent with that of biotite-garnet gneiss (8042) from this region and reflects the peak metamorphic condition.

Nearly all of thermo-barometric data are from the southernmost part of the Sangnong zone (Fig. 8). The P-T-time paths of granulite in the mar-

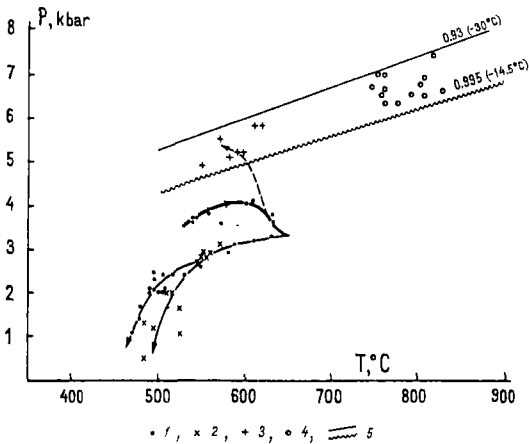


Fig. 8. Conditions and evolution trends of metamorphism and metasomatism in the Machenryong belt. Trend of prograde metamorphism is shown by heavy line, and that of retrograde metamorphism and metasomatism by thin line. 1, metamorphic rocks of the amphibolite facies zone from Haechon, Sangnong and Wondon regions; 2, metamorphic rocks from the Sangnong deposit; 3, metasomatic rocks from the southwestern part of the Sangnong structural zone; 4, granulites of the Kimchaek zone; 5, CO₂ isochores (cf. Fig. 9) in quartz of migmatite leucosomes of Kimchaek (219), corresponding to beginning of continuous row of density (solid line) and frequency maximum (wavy line).

ginal part of the Sangnong zone, and in the Kimchaek zone appear to increase in pressure. However, in the central part of the Sangnong zone, metasomatic rocks related to the ore deposit suggest slight cooling after the peak metamorphism, accompanied by decompression from 4 to 1 kb.

FLUID INCLUSIONS

Fluid inclusions were studied by Vapnik in double-polished section of about 0.2 mm in thickness, using microscope Amplevel and Orthoplan Polar, heating and freezing stages, constructed by Vapnik. Analytical techniques are the same as described by Tomilenko and Chupin (1983) and Roedder (1984). The freezing stage was calibrated using pure organic synthetic substances with the known melting points. The precision of temperature measurements is $\pm 0.5^\circ\text{C}$. Fluid CO₂ inclusions were identified by melting of inclusion

substance after its freezing at -56.6°C (T_m). Specific volume for pure CO₂ inclusions can be determined directly from the homogenization temperature (T_h) by using handbook data on the two-phase region of the CO₂ system (Vargaftic, 1972). The P-V-T diagram for CO₂ based on the data by Shmulovich *et al.* (1982) was used for determining pressure at known temperature and CO₂ isochore. For aqueous inclusions eutectic (T_e) and final melting (T_m) temperatures of ice were established to determine the concentration and composition of salt (Borisenko, 1982; Roedder, 1984). T_h of two and multi-phase inclusions were determined during the heating.

Quartz and garnet of the granulite facies rocks (migmatites, gneisses, leucosomes and granitoids) in all of the studied regions contain pure CO₂ inclusions ($T_m = -56.6^\circ\text{C}$) less than 10 μm in size. T_m drop by 1–2°C occurs in the Kanggye region. Intragrain primary-secondary inclusions are most common, while intergrain secondary ones occur less commonly. In addition, isolated inclusions or their groups are rarely found in the grain centers. They are considered to be primary and earlier than the trail inclusions.

In addition to CO₂ inclusions, N₂ and N₂+CO₂ ones in the form of intragrain planar trail occur in granulites of the Wonsan, Kanggye and Hui-chon regions. The N₂ and mineralized aqueous inclusions are often coeval and secondary (194-3, [γ_3]). The N₂ inclusion commonly homogenizes in gas phase or rarely in liquid. There are several cases of critical homogenization. Freezing of solid phase and melting observed at -68°C to -95°C indicate a presence of CO₂ in the N₂ inclusion. The CO₂ impurity shifts T_h to higher temperature relatively to the critical point of N₂ (-147°C) (Roedder, 1984). Rare H₂O+CO₂ inclusions commonly occur in large granitoid bodies of the Kanggye region [γ_2] and the Kimchaek pegmatites. They homogenize in the gas phase.

Primary-secondary and often secondary aqueous single or two-phase inclusions with variable mineralization occur in general. Te of these

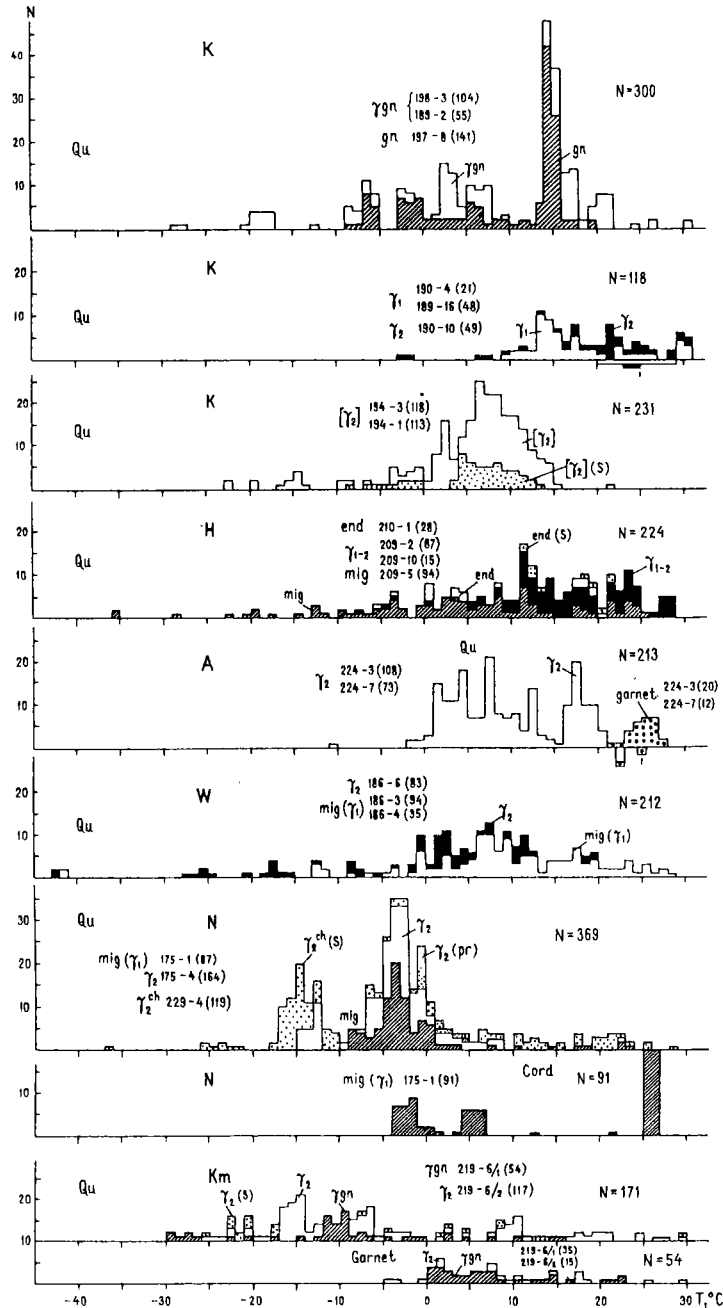


Fig. 9. Histograms of homogenization temperature (T_h) for the CO_2 inclusions in quartz (Qu), garnet and cordierite (Cord). Studied regions : Kanggye (K), Huichon (H), Anju (A), Wonsan(W), Nampo (N), Kim-chaek (K). N: number of the investigated inclusions; homogenization in liquid and gas : upward and down-ward of the abscissa, respectively. Rock symbols : gn, gneiss, mig- migmatite, mig (γ_1), migmatite with early leucosomes, 1-leucosomes of generation 1 in the stromatic migmatite, γ_2 -leucosomes in network migmatites of generations 3 and 4, gn- granite-gneiss, end- enderbite, γ_2^h - crosscutting leucosome with orthopyroxene, $[\gamma_2]$ - large granite bodies of the second generation. Sample numbers and number of the investigated inclusions (in bracket) are shown. T_h concerns the predominant primary-secondary inclusions. Data from secondary (s) and primary (pr) inclusions are also shown.

inclusions ranges from -30 to -55°C , rarely to -60°C , suggesting Ca and Na chloride mineralizations. These results indicate that there are two types of aqueous inclusions: the first type corresponding to salinity greater than 30 wt % eq. NaCl and the second one with low mineralization (<10 wt % eq. NaCl).

The main attention was given to study CO_2 -inclusions. The results are shown as histograms for Th of the CO_2 -inclusions (Fig. 9) in quartz, garnet or cordierite from gneisses, migmatite leucosomes early and late, granite-gneisses and the large granite body. Th corresponds to density (or specific volume) of the inclusion. Th was measured mainly for the primary-secondary inclusions, rarely for secondary ones and in single case (174-4) for primary ones. Th of the primary-secondary inclusions ranges from -25°C to $+30^{\circ}\text{C}$. The denser inclusions of primary-secondary nature are often characteristic for network leucosomes intersecting early migmatite layers (Fig. 9 N, γ_2) and for large granite bodies (Fig. 9 K, $[\gamma_2]$). The ranges of density for the CO_2 inclusion in quartz and cordierite coincide (Fig. 9 N, mig), while garnet contains the reequilibrated inclusion with low density (Fig. 9 A, K_m). The same relationship is known for other granulites (Touret and Olsen, 1985; Touret and Hansteen, 1988; Vapnik and Sedova, 1986; Vapnik, 1988).

Densities of the secondary CO_2 inclusions in intrusive rocks are usually smaller and more restricted than those of the primary-secondary inclusions in the same sample (Fig. 9 K $[\gamma_2]$, H, end). However, in leucosomes where the overprinted schistosity accompanies fibrolite, muscovite and biotite, secondary inclusions have higher densities than the earlier, primary-secondary ones (Fig. 9, N $\gamma_2^{\text{th}}(\text{S})$). Such relationships for inclusions of different density were pointed out by earlier workers (Touret and Hansteen, 1988; Berdnikov, 1987).

The CO_2 isochores, corresponding to either the separate densest inclusion (minimum T_h) or low density group in the continuous spectrum of in-

clusions ($T_h = -30-0^{\circ}\text{C}$), intersect a P-T box of the granulite facies condition. The isobaric trend of some granulites is confirmed by the CO_2 inclusions: secondary inclusions have higher densities than primary-secondary ones. The isochores for the frequency maxima of Th ranging from 0 to 30°C do not intersect the granulite facies condition, because of the inclusion transformation or the growth during retrograde stage (at $T < 500^{\circ}\text{C}$ and $P < 2-3$ kb). The $\text{H}_2\text{O}-\text{CO}_2$ and N_2 inclusions form during this retrograde stage. The P-T path of the Wonsan granulite is delineated from the intersection point between liquid line for 53.5 mol % NaCl in the NaCl-H $_2\text{O}$ system (Roedder, 1984), established for multiphase inclusions with the halite crystal, and the isochore of the densest CO_2 inclusion (Fig. 7). Both inclusion types are coeval. The isobaric cooling proceeds approximately to this intersection point according to mineral thermobarometry. The metamorphic evolutionary paths are different among blocks of northern and southern parts of the country: prolonged isobaric trends are characteristic for the latter. This isobaric cooling may significantly increase the density of the later, secondary inclusions. Similar tendency is recognized for the Nampo granulite until the frequency maxima appear in low Th range of the CO_2 inclusions.

DISCUSSION AND CONCLUSIONS

Our data on Archean and Proterozoic high grade metamorphic rocks from the Nangnim block, being the eastern part of the North China granulite belt, and from the Chungsan and Macheonryong belts allow us to delineate both paleogeotherms and evolutionary petrogenetic regime of each metamorphic terrane.

The earliest metamorphic event in the Nangnim block was the formation of relatively low pressure granulites under the relatively high geothermal gradient. This event was preserved at the metamorphic peak at the pressure of 5–6 kb. The same environment predominated in the

Wonsan and Haeju windows of the Chungsan belt. In the Nampo region, however, the peak temperature reached 6.5–7 kb, suggesting a lower geothermal gradient. The maximum pressure often occurred during cooling. Nevertheless, the early events within the different blocks were likely to be contemporaneous. Thus, inhomogeneous heating of the crust and localization of the heat flow are apparent.

Retrograde P-T-time paths are diverse, but have similar features. Cooling occurs either nearly isobarically or with increasing pressure. Both suggest the lowering of the geothermal gradient. The P-T-time paths are often parallel to the isochores of the CO₂ inclusion. The isothermal decompression is apparent only for Sangnong zone of the Macheonryong belt. However, in its SW part near the boundary with Nangnim block, this belt experienced a cooling with increasing pressure that was accompanied by intensive acid leaching.

The general tendency of cooling at constant or rising pressure was supported by not only mineral thermobarometers but fluid inclusions. The densest inclusions were identified as secondary or primary-secondary ones, and formed during retrograde stage of metamorphism. Thus, the high P estimate during cooling is certain. In addition, the P estimate of the Gr-Sil-Cord barometer higher than that of the Gr-Cord-Bt one might be explained because sillimanite is commonly secondary.

In this section, we will relate the P-T-time paths to the geodynamic environment. Isobaric cooling often results from the demise of a heat source such as mantle diapir upwelling to the lower crust. Because positive thermal anomalies appear during the early stage, hypothesis of pure dying of a heat source is unacceptable. The granulite facies rocks recrystallized after the peak metamorphism, the migmatite formation and the emplacement of para-autochthonous and allochthonous bodies related to multi-stage folding and shear zone. Therefore, tectonic movements accompanying the cooling varied in direction and rate. This variation

may account for the diversity of P-T-time paths. A part of the rock mass uplifts, while another part sinks and juxtaposition of hot and cold rocks results in the cooling of the high temperature rocks. Such thermal effects are often present in the tectonic belt with nappe-thrust structure (Glebovitsky, 1991) and are identified in the Chungsan belt.

In granulites of both the Chungsan belt and the Nangnim block all P-T-time loops pass through a P-T range of 625–674°C and 5.0–6.5 kb. This range is the peak condition of the kyanite-sillimanite type metamorphism which defines the Chungsan belt. Consequently, all of the retrograde metamorphism occurred at the same P-T condition, and at least in early Proterozoic the Chungsan belt and the Nangnim block were a single terrane. The Chungsan complex partly represents the strongly reworked moderate and low-P granulites. These results are consistent with the recent Proterozoic Rb/Sr age of the Nampo granulites (Gorokhov *et al.*, 1993).

Both high-P granulite and amphibolite facies rocks experienced the cooling accompanied by more or less significant decompression (Figs. 6 and 7). Decompressional cooling is suggested by the formation of andalusite in staurolite-kyanite schists and overprinting metasomites. This cooling process also accounts for the formation of numerous, reequilibrated CO₂ inclusions with low density.

Variable P-T-time paths of the Macheonryong belt suggest a metamorphism of the andalusite-sillimanite type. In the Sangnong and Wondong deposit regions, P-T-time paths resulted from uplifting related to the emplacement of granite and granite-gneiss plutons at the center of positive thermal anomaly zone. This uplift occurred so rapidly that pressure decreased almost isothermally. In addition, isobaric cooling is apparent at the central part of zone. In the southwestern marginal part the cooling was accompanied by increasing pressure, that may have compensated the uplifting of the central zone.

The Kimchaek metamorphic complex located in the northeastern margin of the Machenryong belt has special features. Paleo-geotherms sharply differ from those described in the above. There is no evidence that Machenryong and Kimchaek complexes experienced the same retrograde evolution. Moreover, eclogite-like rocks formed instead of mafic granulites with increasing pressure and decreasing T. Magnesian skarns of the Pkhsu deposit formed at pressures greater than 7 kb, as suggested from garnet-orthopyroxene-clinopyroxene schists and Al-rich gneisses. Although the Kimchaek and Macheonryong complexes have similar Rb/Sr ages (Gorokhov *et al.*, 1994), the Kimchaek complex is a separate tectonic block different from the Macheonryong belt. The former complex may represent a large nappe thrust over the NE Archean plate.

In conclusion, the earliest event in both northern and southern parts of the country belonging to the Sino-Korean and Yangtz platforms, respectively, was the formation of intermediate and low-pressure granulite rock complexes representing the easternmost part of the North China granulite belt. These granulites generally experienced the cooling at constant or with increasing pressure, suggesting a transition from high to moderate or low geothermal gradient in the whole area of the Nangnim block and the Chungsan belt. Almost complete reworking of the earlier granulites occurred under the amphibolite facies condition of the kyanite-sillimanite facies series. The anti-clockwise P-T-time path may result from thrusting and thickening of crust in the collisional zone.

ACKNOWLEDGEMENT

We thank Choi Von-Cen, Kim Ryo-Su and Kim Song-A for their assistance throughout this project. We also thank M. Cho, S.-T. Kwon and E.Y. Jeon for refining English expression of the manuscript.

REFERENCES

- Berdnikov N.V., 1987, Thermobarogeochemistry of Precambrian metamorphic complexes of the Far East. Nauka-Press, 117p (in Russian).
- Borisenko A.S., 1982, Salt-composition analysis of the solution inclusions from minerals by cryometrical method. In: Using of thermo-barometrical methods at prospecting and study of ore deposits. Nedra-Press, 37-46. (in Russian).
- Field excursion guidebook on the ore deposition in Liaodong Peninsula, 1985, The Organizing Committee, International Symposium on Metallogeny of the Early Precambrian. Changchun, China, 53p.
- Glebovitsky V.A., 1991, Vertical zonality of endogenic processes and sections of the Earth crust in Precambrian structures of the Baltic shield. In: The problems of geological and geophysical data interpretation. Nauka-Press, 9-24 (in Russian).
- Glebovitsky V.A. and Drugova G.M., 1979, Facies and subfacies boundaries for poor in Ca rocks from garnet-biotite thermo- and barometrical data. In: Problems of Physical-Chemical Petrology. Vol. 1, Nauka-Press, 46-59 (in Russian).
- Glebovitsky V.A., Kosoi A.L. and Nagaitsev Yu.V., 1972, Temperature and pressure determination from mineral composition in paragenesis biotite-garnet-cordierite. Doklady AN SSSR, 204, N 2, 948-951 (in Russian).
- Glebovitsky V.A., Vapnik Ye.A. and Sedova I. S., 1990, Fluid regime of granite formation in zones of ultrametamorphism. Geologiskiy Zbornik, Geologica Carpatica. 41, N 6, 641-652.
- Gorokhov I.M., Glebovitsky V.A., Bushmin S.A. et al., 1993, Rb-Sr age of the early Precambrian metamorphic rocks of Northern Korea. Stratigraphy and Geological Correlations, N 3, 26-37.
- Marakushev A.A., Kim Kheck-Tze, Kim Khe-Noo and Mishkin M.A., 1966, Precambrian metamorphic complexes of Northeastern Korea and the South of the Far East and ore deposits related to them. In: Geologicheskoye Stroeniye Severo-vostoka Koreyi i Yuga Primoria. Nauka-Press, 9-123 (in Russian).
- Lavrentyeva I.V. and Perchuk L.L., 1990, Orthopyroxene-garnet geothermometer: experiment and theoretical development of the data base. Doklady AN SSSR, 310, N 1, 179-182 (in Russian).
- Newton R.C., 1986, Fluids of granulite facies metamorphism. In: Walther J.T. and Wood B.J. (Eds). Fluid-rock Interaction and Metamorphism, Springer Verlag, Berlin, 36-59.
- Perchuk L.L., 1989, Confirmation of some Fe-Mg geothermometers on the base of Nernst's law. Geokhimiya, NS, p. 611-622.

- Perchuk L.L., 1989, P-T-fluid regime of metamorphism and related magmatism with specific reference to the granulite facies in Sharyzhalgay complex of Lake Baikal. In: Daly S.J., Cliff K.A., and Yardley B.W.D. (Eds). Evolution of Metamorphic Belts. Geological Society of London. Special Publication, 43, 275-291.
- Perchuk L.L., Aranovich L.Ya., Podlesslii K.K., Lavrentyeva I.V., Gerasimov V.Yu., Fedkin V.V., Kitsul V.I., Karsakov L.P., and Berdnikov N.V., 1985, Precambrian granulites of the Aldan shield, Eastern Siberia, USSR. *Jour. Metamorphic Geol.*, 3, 265-310.
- Ren Jishun, Jiang Chunfa, Zhang Zhegkun, and Qin Deyu, 1987, Geotectonic evolution of China. Science Press, Beijing, Springer Verlag, 203p.
- Roedder E., 1984, Fluid inclusions. *Reviews in Mineralogy, Mineral. Soc. Am.*, 12, 644p.
- Sedova I.S. and Glebovitsky V.A., 1984, Ways of evolution of the ultrametamorphic zones, *Izv. AN SSSR, set. geol.*, N 11, 25-36.
- Sengupta F., Desgupta S., Battacharya P.K., and Mukherjee M. 1990, An orthopyroxene-biotite geothermometer and its application in crustal granulites and in mantle-derived rocks. *Jour. Metamorphic Geol.*, 8, 191-197.
- Shmulovich K.I., Tereschenko E.N., and Kalinichev A.G., 1982, A state equation and isochores of unipolar gases till 2000K and 10 GPa. *Geokhimiya*, 11, 1598-1614 (in Russian).
- Tomilenko A.A. and Chupin V.P., 1983, Thermobarogeochemistry of metamorphic complexes. Nauka-Press, 200 (in Russian).
- Touret J., 1986, Fluid inclusions and pressure-temperature estimates. In: H.C. Helgeson (Ed) *Chemical Transport in Metasomatic Processes*. NATO ASI series, ser. C, Reidel Publ., 218, 91-114.
- Touret J. and Hansteen T., 1988, Geothermobarometry and fluid inclusions in a rock from the Dodbetta charnockite complex Southwest India. *Rendiconti Della Societa Italiana Di Mineralogia*. 43, 65-82.
- Touret J. and Olsen S., 1985, Fluid inclusions in migmatites. In: Ashworth J.R. (Ed). *Migmatites*. Blackie Publ., London, 265-286.
- Vapnik Ye.A., 1988, Dynamics of development of Ladogian granitoid complexes from fluid inclusion studies. *Zapiski Vses. Miner. Obschestva*. CXVII, 2, 305-318.
- Vapnik Ye.A. and Sedova I.S., 1986, Pressure conditions and fluid compositions during ultrametamorphism in the Aldan megablock. *Inter. Geol. Rev.*, 28, 11, 1293-1305.
- Vargaftik N.B., 1972, Handbook on physical features of gases and liquids. Nauka-Press, 197p (in Russian).

(책임편집 : 조문섭)

한반도 북부의 백립암

V.A. 글레보비츠키¹, I.S. 세도바¹, S.A. 부시민¹, Ye.A. 바프닉¹, A.K. 부이코¹

¹Institute of Precambrian Geology and Geochronology of Russia Academy of Science, emb. Makarova 2, St. Petersburg 199034, Russia.

요 약: 이 논문은 한반도 북부의 백립암 복합체에 대한 연구결과를 제시한다. 이 복합체는 지역에 따라 북부지역의 낭림 블록, 동부 지역의 마천령대내 김책 누대, 그리고 남부 지역의 상부 원생대의 구조 중에 산재되며 인접 지역의 이름을 따라 원산, 남포, 해주 백립암이라 명명된 원도우들로 세분된다. 이들 백립암 복합체에서는 다단계 변형 작용과 화강암 형성을 포함하는 변성 및 미그마타이트작용이 인지된다. 광물 지은 지압계와 유체포유물 연구 자료는 전진 및 후퇴 변성작용 동안의 온도와 압력 조건의 진화 경로를 확립시키는데 도움을 준다. 어떤 경우는 백립암 변성작용의 최대 온도와 압력은 약 800°C와 약 5.6-6 kb인 것이 특징적이다. 후퇴변성작용의 진화는 일정하거나 혹은 7-8 kb 정도까지 증가하는 압력하에서의 냉각 과정을 포함하는데, 이는 높은 지온구배에서 중간 또는 낮은 지온구배로의 전이에 해당한다. 나중에 이 냉각 과정은 3-4 kb로의 상당한 압력 하강에 수반되어 일어났다.

핵심어: 백립암, P-T-t 경로, 유체포유물